PB-229 698

THE INFLUENCE OF AXIAL DISPERSION ON THE FIXED BED ABSORPTION OF THE HYDROGEN CHLORIDE-CHROMIUM OXINATE SYSTEM

Eugene E. Berkau, et al

Vanderbilt University
Nashville, Tennessee

1963

DISTRIBUTED BY:

NTIS

National Technical Information Service
U. S. DEPARTMENT OF COMMERCE
5285 Port Royal Road, Springfield Va. 22151

WP00871-03

PB 229 698

THE INFLUENCE OF AXIAL DISPERSION ON THE FIXED BED ADSORPTION OF THE HYDROGEN CHLORIDE-CHROMIUM OXINATE SYSTEM

By

Eugene E. Berkau, Gerald T. Fisher and Mark M. Jones
Departments of Chemical Engineering and Chemistry
Vanderbilt University
Nashville, Tennessee

LIST OF REFERENCES

1. Anzelius, A., Z. Angew. Math. U. Mech. 6, 291-294 (1926).

2. Brunauer, The Adsorption of Gases and Vapors, Princeton University Press, Princeton, 1945.

3. Brunauer, Emmett, Teller, J. Am. Chem. Sci. 60, 309 (1938).

4. Brunauer, Deming, Deming, and Teller, J. Am. Chem. Soc. 62, 1723 (1940).

5. Ceaglske, N. H., Automatic Process Control for Chemical Engineers, John Wiley and Sons, New York (1959).

6. DeBoer and Zwikker, Z. Physik. Chem. B3, 407 (1929).

7. De Saussure, Gilberts' Ann. Physik. 47, 113 (1814).

8. De Vault, D., J. Am. Chem. Soc. 65, 532 (1943).

9. Edeskuty, F. J., and N. R. Amundson, J. Chem. Phys. 56, 148 (1952).

10. Fick, Ann. Physik. 94, 59 (1855).

11. Freundlich, Colloid and Capillary Chemistry, London, (1926).

12. Head, F. E., "Determination of the Performance Function of Mixing in a Model of a Tubular Reactor," Master's Research Thesis, St. Louis University, 1959.

13. Hougen, O. A., and Marshall, W. R., Jr., Chem. Eng. Progress, 43, 197 (1947).

14. Jones, M. M., Dandh, K. V., and Fisher, G. T., J. Inorg. Nucl. Chem. 26, 773 (1964).

15. Krenkel, P. A., and Orlob, G. T., Journal of the Sanitary Engineering Division, Proceedings of the American Society of Civil Engineers, 88, 53 (March, 1962).

16. Langmuir, J. Am. Chem. Soc. 38, 2267 (1916), 39, 1883 (1917), 40, 1361 (1918).

17. Levenspiel, O., Chemical Reaction Engineering, John Wiley and Sons, New York, 1962.

18. Magnus, Z. Physik. Chem. A142, 401 (1929).

19. Maguire, K. D., and Jones, M. M., J. Am. Chem. Soc. 84, 2316 (1962).

20. Mantell, C. L., Adsorption, McGraw-Hill, New York, 1951.

21. Masamune, S., and Smith, J. M., Ind. and Eng. Chem. (Fund Quarterly) 3, 179 (1964).

22. Masamune, S., and Smith, J. M., A. I. Ch. E. Journal 11, No. 1, 34 (1965).

23. Mickley, H. S., Sherwood, T. R., and Reed, C. E., Applied Mathematics in Chemical Engineering, McGraw-Hill Book Company, New York, 1957.

24. Murfree, J. A., Jr., "Construction and Operation of The Gas Chromatography Equipment in the Radiation Research Laboratory at Vanderbilt University," Ph. D. Thesis, Vanderbilt University, 1961.

25. Nusselt, W. Z., Ver. dent. Ing. 55, 2021 (1911).

26. Patrick and McGavack, J. Am. Chem. Soc. 42, 945 (1920).

27. Paynter, M. H., A Palimpsest on the Electronic Analog Art, Geo. A. Philbrick Researches, Inc., Boston (1955).

28. Polanyi, M., Verh. dent. Physik. Ges. 16, 1012 (1914).

29. Polanyi, M., Verh. dent. Physik. Ges. 15, 55 (1916).

30. Rosen, J. B., J. Chem. Phys. 20, 387 (1952).

31. Rosen, J. B., Ind. Eng. Chem. 46, 1590 (1954).

32. Stanton, Ralph G., Numerical Methods for Science and Engineering, Prentice Hall, Inc., Englewood Cliffs, New Jersey, pp 116, 117.

33. Thiele, E. W., Ind. Eng. Chem. 38, 646 (1956).

34. Thomas, H. C., J. Am. Chem. Soc. 66, 1664 (1944).

35. Thomas, H. C., J. Chem. Phys., 19, 1213 (1951).

36. Van Bemmelen, Mitt. landw. Wersuchsstation 35 (1888).

37. Whitman, W. G., Chem. Met. Eng. 29, 146-148 (1923).

38. Willard, H. H., Merritt, L. L., Jr., Dean, J. A., Instrumental Methods of Analysis, D. Van Nostrand Company, Inc., Princeton (1963).

39. Zsigmondy, Z. anorg. Chem. 71, 356 (1911).

List of Figures

Figure 1	Section of Adsorption Cell
Figure 2	Schematic of Experimental Apparatus
Figure 3	Inlet Mole Fraction Versus Breakthrough Time
Figure 4	Concentration Versus Time Since Breakthrough
Figure 5	Adsorption Equilibrium Data
Figure 6	General Module for the Analogue Computer Program
Figure 7	End Module Analogue Computer Program
Figure 8	Experimental and Theoretical Concentration Histories I
Figure 9	Experimental and Theoretical Concentration Histories II
Figure 10	Experimental and Theoretical Concentration Histories III
Figure 11	Effect of Number of Computer Modules on Theoretical Behavior

Nomenclature

B	-	constant in the Freundlich equation
C	-	gas phase adsorbate concentration, g-moles/liter
$\bar{C}$	-	gas film adsorbate concentration, g-moles/liter
C_o	-	adsorbate concentration at z = 0 (boundary condition), g moles/liter
D_g	-	gas phase dispersion coefficient, cm^2/sec.
E	-	solid phase composition, g-moles adsorbate/g-mole solid
N	-	adsorbate molar flux, g-moles/cm^2 sec.
P	-	interfacial area in bed cross section, cm^2
P	-	partial pressure of adsorbate
R	-	partial radius, cm
S	-	adsorbate concentration on the solid surface g-moles adsorbate/g-mole adsorbent
S_i	-	adsorbate concentration in the ith bed increment, g-moles/g-mole
b	-	D_g/ϵ
b'	-	$D_g/\epsilon\Delta z^2$
C	-	C/C_o, dimensionless
C_i	-	value of c in the ith increment of the bed
d	-	u/ϵ
d'	-	$u/\epsilon 2\Delta z$
e	-	$\rho_s/C_o\epsilon$
f	-	$f'C_o$

f' - constants defined by Equation (11) and Model I, II, or III

g - constants defined by Equation (11) and Model I, II, or III

$k_g a$ - gas phase mass transfer coefficient, sec^{-1}

k_1 - absorption rate constant, sec^{-1}

k_2 - desorption rate constant, sec^{-1}

m - constant in the Freundlich equation

n - number of finite bed increment

r - rate of adsorbate mass transfer through the gas film, g-moles/liter-sec.

t - scaled computer time, $\theta/100$ sec

u - linear velocity through bed, cm/sec

z - linear distance in the bed, cm

β - equilibrium constant, Equation (9), dimensionless

ϵ - bed porosity, dimensionless

θ - time, sec

λ - equilibrium constant, Equation (7), liter/g-mole solid

ρ_s - adsorbent bulk density, g-mole/liter

ABSTRACT

The results from a study of the removal of gaseous hydrogen chloride by the solid, metal organic complex, chromium oxinate, in a fixed-bed adsorption column is presented in the form of adsorption curves or exit gas concentration histories. These experimental curves are subsequently compared to the solutions of a theoretical mathematical model representing the adsorption process. The model incorporates axial diffusion, as described by G. I. Taylor. A gas phase mass transfer resistance and a solid phase adsorption-desorption rate were considered as the mechanisms for the adsorption model. The solutions to the mathematical model were generated by an analog computer.

INTRODUCTION

The theoretical mathematical representation of the removal of a component from a gas mixture in a fixed-bed adsorption process requires the description of the mechanisms of mass transfer of the adsorbate from the bulk gas stream onto the surface of the solid adsorbent. These rate controlling mechanisms which were first suggested by Langmuir (4) are:

1. Diffusion of adsorbate to external surface of the solid particle (external diffusion)
2. Diffusion of adsorbate into or along the surface of the solid particle (intraparticle diffusion)
3. Adsorption and desorption of the adsorbate on the solid surface (surface adsorption).

One of the first formulations applied to a fixed-bed adsorption process was that presented by Marshall and Hougen (13) which assumes that external diffusion or surface adsorption is the controlling mechanism. Mathematical solutions have also been developed by Thomas (35), Rosen (30), and Edeskuty and Amundson (9) for the case in which intraparticle diffusion is the dominating mechanism. The theoretical treatment of the combined resistances of intraparticle and external diffusion was first obtained by

Rosen (31). Masamune and Smith (21,22) solve the additional two-resistance and the general three-resistance cases and summarize all previous mathematical formulations for a fixed-bed adsorption process where the adsorbent particles are considered to be spherical.

A simplifying assumption common to all these mathematical developments is that axial diffusion or back-mixing of the adsorbate in the gas mixture is negligible or non-existent. Such an assumption prevents the solutions of the theoretical models from predicting the tailing which is exhibited in experimental adsorption concentration data presented in this paper. The mathematical model which is proposed will consider the mass transfer controlling resistances of external diffusion and surface adsorption and in addition the back-mixing of the adsorbate in the gas stream. The machine solutions to this model are presented and compared to a set of experimental curves obtained from the adsorption process studied.

EXPERIMENTAL

The solid adsorbent was tris(8-hydroxyquinolinato) chromium(III) or chromium oxinate and was prepared by a procedure available in the literature (19). The solid was reddish-brown in color and its particle size as determined by separation in a set of Tyler standard screens was between 74 and 104 microns.

The adsorbate utilized was anhydrous hydrochloric acid, and the inert component of the gas mixture, helium. These gas sources were standard gas cylinders supplied by Matheson, of commercial purity. The mole fractions of hydrogen chloride ranged from 0.50 to 0.053 under a total average pressure of not more than 1 psig which was caused by a pressure drop in the adsorbent bed. These figures correspond to total gas flow rates ranging from 9.74 to 4.36 ml/sec. The helium rate in all instances was constant at either 4.87 or 4.13 ml/sec.

The initial temperature of the system preceding an experiment was either 25°C or 35°C. The lengths of the experiments ranged from 30 min. to 5 hrs. An experiment was never concluded until the output gas concentration was equal to or greater than 90 percent of the input concentration.

Although the system was operated under anhydrous conditions, the experimental equipment was designed primarily from consideration of the corrosiveness of concentrated HCl. Because of its inertness, polyvinyl chloride pipe and fittings were used almost exclusively, and clear Lucite tubing was the construction material for the wall of the fixed-bed. The reactor itself was initially designed for 90 gm of adsorbent but was subsequently altered for sample sizes of 55 gm when preliminary experiments indicated that the time required to complete low gas concentration experiments would be lengthy. The modification of the reactor volume was accomplished by reducing the bed length from 6 to 4 in. while maintaining the inside diameter at 1.5 in. A scale drawing of the experimental adsorption cell is in Figure 1.

The concentration of the inlet and effluent gas streams to the reactor was monitored continuously by two Gow-Mac thermal conductivity cells. Teflon coated thermistors were used as the sensing elements. The flow rates of the individual gases (HCl & He) were measured by two gas rotameters. A flow diagram of the experimental apparatus is presented in Figure 2.

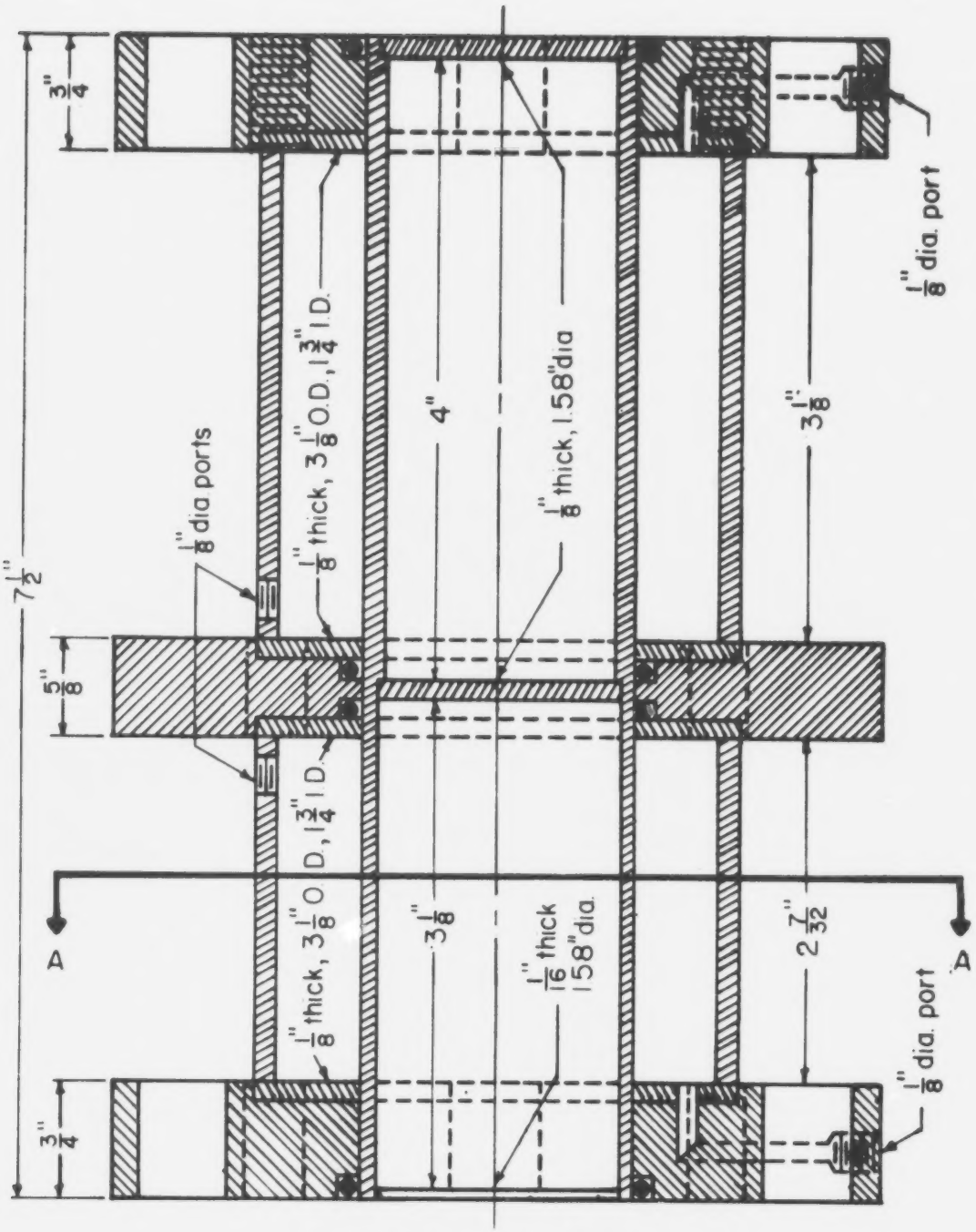

Section AA, See FIGURE 7

FIGURE 1

SECTION OF ADSORPTION CELL

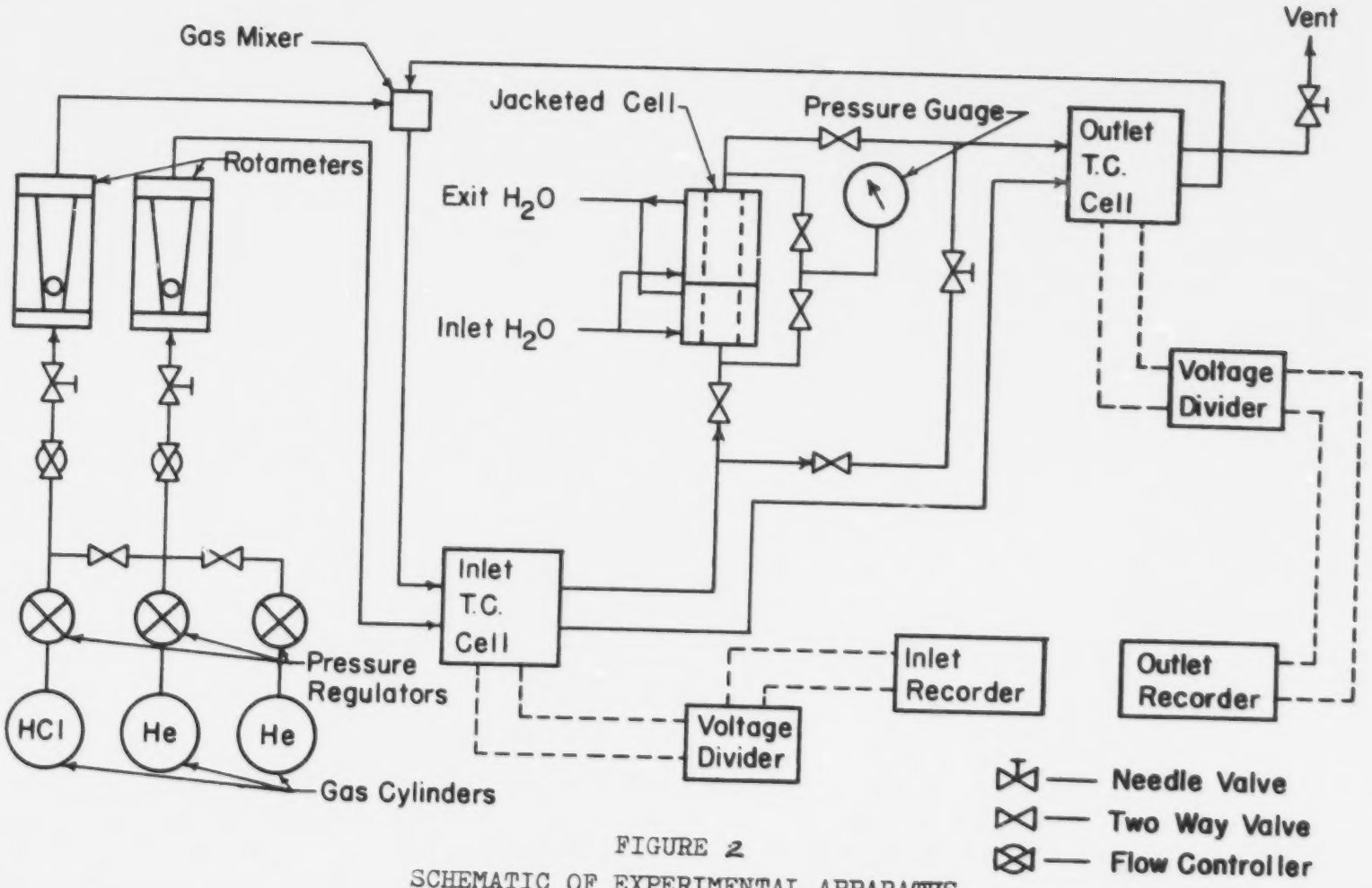

FIGURE 2
SCHEMATIC OF EXPERIMENTAL APPARATUS

EXPERIMENTAL RESULTS

The experimental results which are generally used to characterize a fixed-bed adsorption process are the output gas concentration versus time data. The most valuable information that can be obtained from these data is the breakthrough time. This term will be defined as the time required for the adsorbate to become measurable in the exit gas stream. Of almost equal importance are the adsorption equilibrium data which are usually more accurately determined from non-flow studies but in this case were estimated from the fixed-bed adsorption results. The factors which must be considered because of their influence on these data are the input gas concentration, sample size, temperature, pressure, and particle size.

A summary of the experimental conditions of temperature, pressure, sample sizes, and hydrogen chloride concentration and flow rates is tabulated in Table 1. Although the initial temperatures of the system were maintained at 25°C or 35°C, subsequent temperature rises were recorded. These temperature rises ranged from 7°C to greater than 50°C for corresponding inlet hydrogen chloride mole fractions of 0.053 to 0.50. Corresponding experiments made under the same operating conditions except base temperatures provided

TABLE 1

EXPERIMENTAL CONDITIONS

Experiment Number	Inlet HCl Mole Fraction	Inlet HCl Flow (ml/sec)	Sample Size (gm)	+Temperature Rise (°)	Average Pressure (psig)
*2A1	0.363	2.78	83.08	--	15.7
*2A2	0.363	2.78	85.60	--	15.7
2A3	0.363	2.78	57.10	--	--
*3A1	0.245	1.47	83.65	--	15.7
*3A2	0.245	1.47	83.00	32.8	15.7
3A3	0.245	1.47	56.70	--	--
*5A1	0.500	4.87	90.30	30.6	--
5A2	0.500	4.87	56.20	>40.0	--
8A	0.085	0.45	87.10	7.0	15.9
9A	0.102	0.48	55.30	8.0	14.8
9B1	0.102	0.48	56.80	8.6	14.8
9B2	0.102	0.48	56.65	11.2	14.8
11A1	0.076	0.34	57.30	10.0	14.9
11A3	0.076	0.34	56.90	10.0	14.9
11B1	0.076	0.34	57.70	7.5	--
11B2	0.076	0.34	56.85	7.5	--
13A	0.128	0.61	57.20	15.7	15.4
13B	0.128	0.61	57.30	12.3	15.4
14A	0.053	0.23	54.75	9.8	15.4
15A	0.198	1.20	56.10	34.0	--

*Water from a temperature bath at 25°C was circulated through the reactor jacket throughout these experiments.

+Experiment numbers containing "A" refer to initial temperature of approximately 25°C and "B", 35°C.

adsorption curves which were not significantly different, and therefore the experimental results were assumed to be independent of temperature over the range in which the studies were made.

The pressure drop within the fixed-bed varied between 0 and 1.2 psi or 14.7 and 15.9 psia. Since this variation was small with respect to the total absolute pressure, the adsorption experiments were assumed to have been operated under isobaric conditions, the average pressure being 15.0 psia.

The adsorbent sample size of 85 gm used in the high adsorbate concentration experiments was changed to 55 gm in order to reduce the time required to conclude the lower concentration studies. The particle size of the adsorbent was between 74 and 104 microns.

In Figure 3 is shown the variation in the break-through times with the inlet gas concentration. It is seen that as the adsorbate concentration decreased from 0.50 to 0.053, the break-through times increased from 5.0 to 32.5 min.

The experimental adsorption curves are presented in Figure 4 as plots of exit gas concentration versus time since break-through period. These curves indicate that the rate

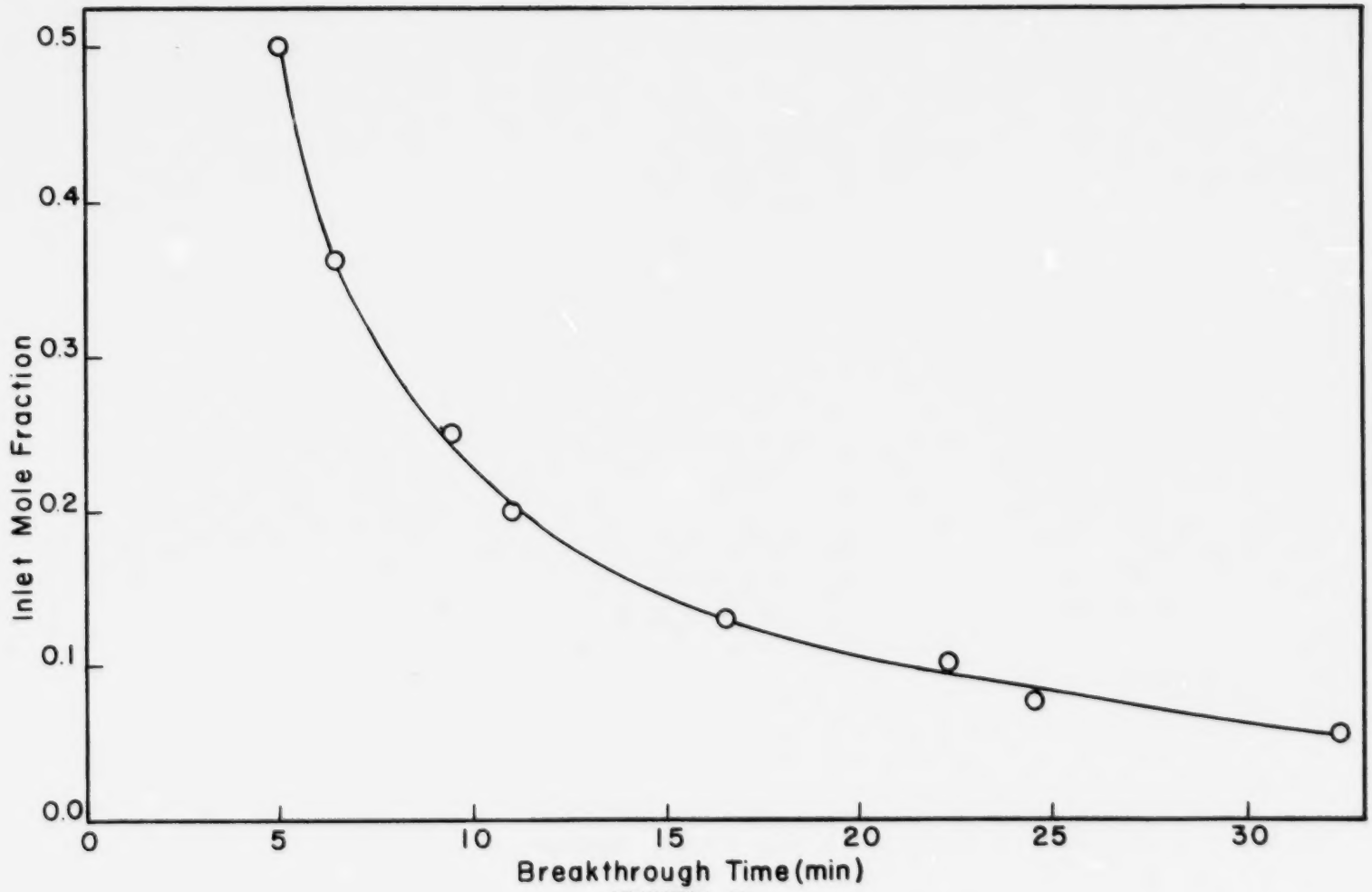

FIGURE 3

INLET MOLE FRACTION VERSUS BREAKTHROUGH TIME

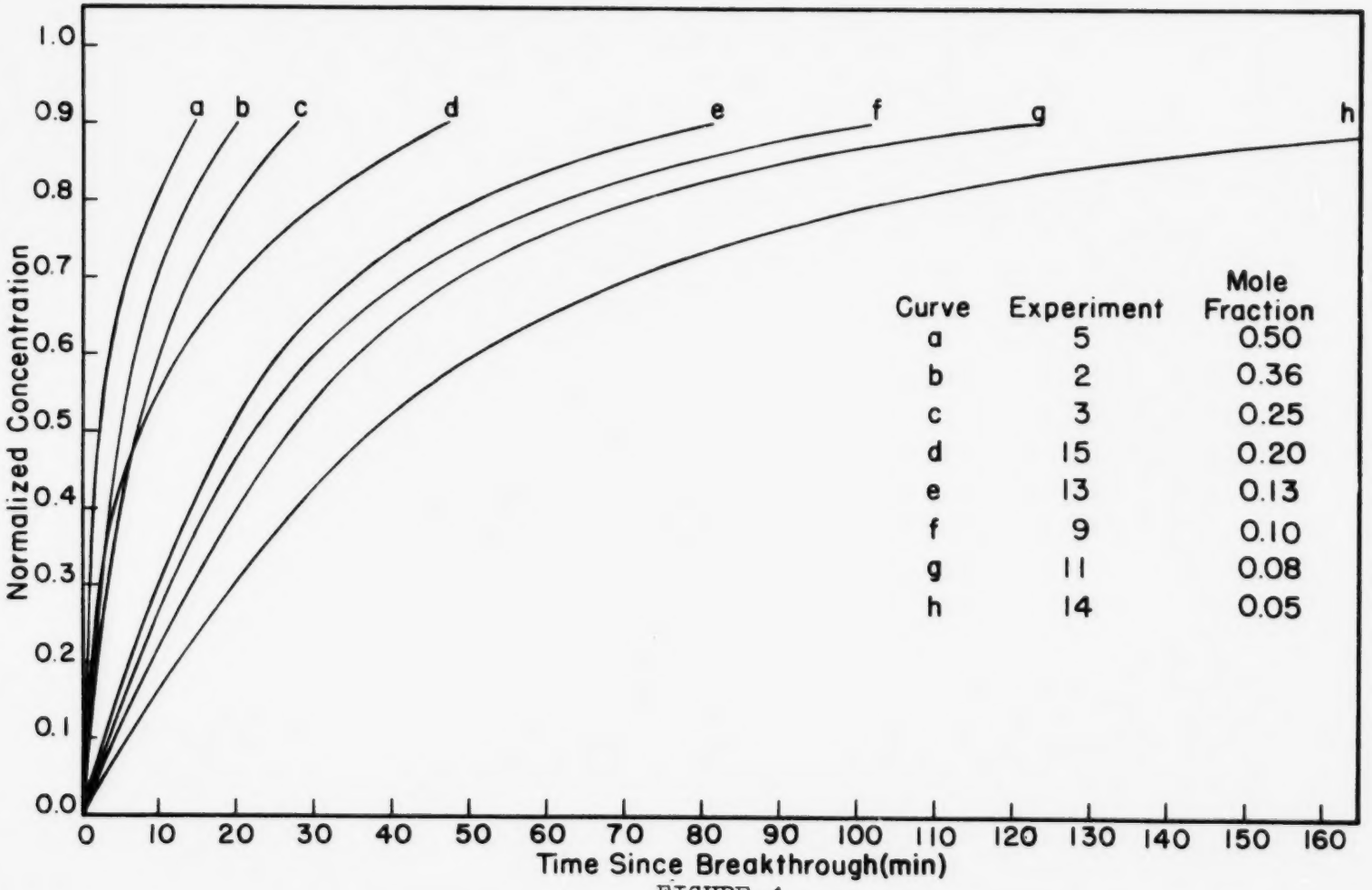

FIGURE 4

CONCENTRATION VERSUS TIME SINCE BREAKTHROUGH

of change of concentration of hydrogen chloride in the exit gas stream decreased with decreasing inlet adsorbate concentration. This in essence is the same as lowering the partial pressure of the adsorbate in the gas mixture and hence decreasing the rate of adsorption. This effect is consistent with the properties of a physical adsorption process.

The reversibility of the fixed-bed adsorption process was investigated in the initial experiments. The method employed was to allow pure helium to pass over the essentially hydrogen chloride saturated bed at the same flow rate as in the preceding adsorption experiment and record the output concentration. The results indicated that the process was reversible with an initially rapid desorption rate, followed by a very slow loss of material from the bed. This evidence was also indicative of a physical adsorption process.

The adsorption equilibrium data was obtained from the exit gas concentration histories which were recorded in raw form as ml/sec of hydrogen chloride in the exit gas stream versus time. By subtracting the hydrogen chloride flow rate leaving (ml/sec) from that entering, hydrogen chloride absorbed versus time curves were obtained. From these curves the adsorption equilibrium data could be calculated with a

knowledge of the temperature and pressure of the system. This data is presented in Figure 5 along with the curve obtained from the empirical Freundlich exponential equation, which is often used to represent adsorption equilibrium data. The form of the equation used was

$$E = B(\bar{P})^{1/m} \quad .$$

The values of B and m which gave the desired fit to the experimental data were B = 0.0367 and m = 0.815.

The reproducibility of the experimental adsorption curves was observed under several sets of operating conditions. The greatest deviation was found to be 12.5 percent and the minimum, 3.0 percent. These values were obtained considering the high and low base temperature experiments together.

THEORY

To predict the change in concentration of a fluid stream and a bed of adsorbent during an adsorption process, it is necessary to obtain an expression which relates concentration to time and distance for both the fluid (in this case the gas) and the solid phases. In order to write such an expression the following physical picture of the adsorption mechanism is presented.

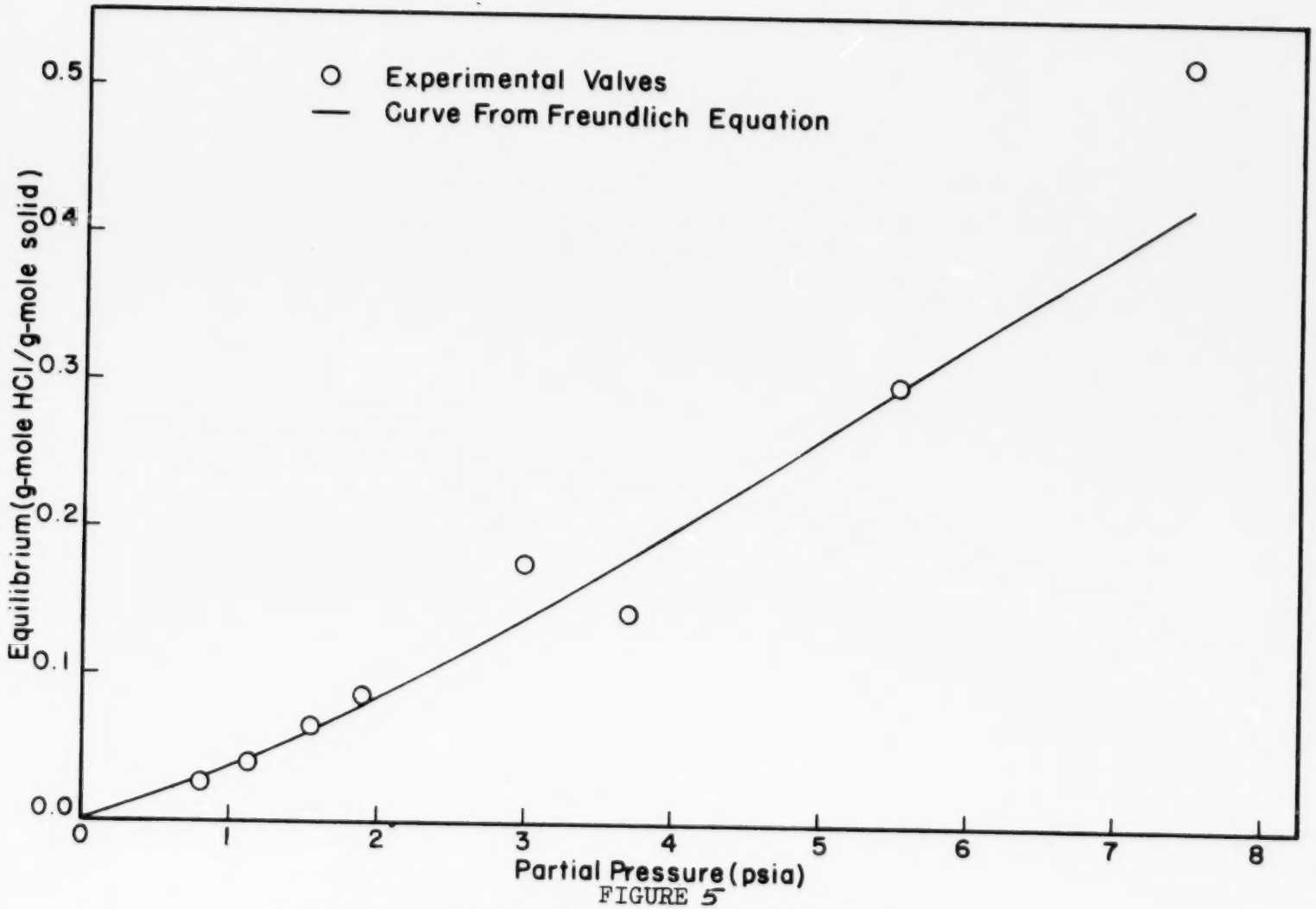

FIGURE 5

ADSORPTION EQUILIBRIUM VERSUS PARTIAL PRESSURE

The gas mixture composed of the adsorbate and inert components is considered to pass through the void spaces between the solid particles in the packed bed. The adsorbate becomes concentrated in the adsorbent at the entrance of the bed. The effluent from this section retains very little of the adsorbate, and hence only a small degree of adsorption occurs throughout the rest of the column. As the entrance of the bed approaches saturation, the adsorption process continues up the bed in what has been called an adsorption wave (8,33,34). While the adsorption wave is proceeding through the adsorbent, the effluent from the bed is relatively free of adsorbate. When the wave reaches the exit, the concentration of the adsorbate increases rapidly until the outlet adsorbate concentration approaches that of the inlet gas stream. The time required for the adsorption wave to reach the exit of the column is known as the breakthrough period. The outlet gas concentration approaches the inlet value slowly as equilibrium or bed saturation is gradually approached. When saturation of the adsorbent is essentially complete, no further concentration changes are observed. The amount of equilibrium adsorption is the same as that which would have been obtained in a static experiment under similar operating conditions.

The adsorbate transfer between phases occurs from the bulk gas stream to a stagnant gas film which encompasses and in some cases intermingles with the solid particles. If the gas film is assumed to surround the solid particles, the adsorbate is then considered to simply adsorb and desorb on the external surface of the solid. In the other situation, adsorbate molecules are assumed to diffuse into the interstices of the solid particles where adsorption and desorption occur on both the external and internal surfaces. The latter case will not be examined in this paper.

To describe the changes in concentration of the gas stream, three major assumptions are made. The first of these is that plug flow in the gas stream exists and that back-mixing of adsorbate can be represented mathematically analogous to Fick's Law describing molecular diffusion. Assuming such a relationship, back-mixing or the molar flux of the adsorbate in the z-direction can be represented as

$$N = -D_g \frac{\partial C}{\partial x}$$

The second assumption is that the rate of mass transfer of the adsorbate across the gas film resistance can be described by the expression

$$r = k_g a \, (C - \bar{C})$$

Finally, the rate controlling transfer mechanisms of adsorption and desorption in the solid phase and surrounding stagnant gas film are considered to be directly proportional to the concentration of the adsorbate. Stated mathematically

$$\text{Rate of adsorption} = k_1\bar{C}$$

$$\text{Rate of desorption} = k_2 S$$

where k_1 and k_2 are the adsorption and desorption rate constants and S is the concentration of the adsorbate on the solid surface.

If the preceding relationships are assumed to apply, then mass balances in the direction of gas flow over an arbitrary differential section in the fixed-bed reactor can be written. Mass balances over the gas phase, solid phase and stagnant gas film, and solid phase lead to the differential equations

$$\epsilon \frac{\partial C}{\partial \theta} = D_g \frac{\partial^2 C}{\partial z^2} - u \frac{\partial C}{\partial z} - k_g a(C-\bar{C}) \tag{1}$$

$$P \frac{\partial C}{\partial \theta} + \pi R^2 \rho_s \frac{\partial S}{\partial \theta} = k_g a \pi R^2 (C-\bar{C}) \tag{2}$$

$$\rho_s \frac{\partial S}{\partial \theta} = k_1\bar{C} - \rho_s k_2 S \tag{3}$$

In Equation (2) the quantity P will be considerably less than $\pi R^2 \rho_s$ since it composes only a minute fraction of the cross-section area of the bed. It can therefore be assumed that

$$P \frac{\partial C}{\partial \theta} \ll \pi R^2 \rho_s \frac{\partial S}{\partial \theta}$$

and hence Equation (2) can be reduced to the form

$$\rho_s \frac{\partial S}{\partial \theta} = k_g a \, (C-\bar{C}). \tag{4}$$

Comparing Equation (4) with Equation (3) the identity,

$$k_g a \, (C-\bar{C}) = k_1 \bar{C} - \rho_s k_2 S, \tag{5}$$

can be written. Solving Equation (5) for $\bar{C}$ and substituting the result into Equation (3) leads to the expression

$$\rho_s \frac{\partial S}{\partial \theta} = \frac{k_1 k_g a}{k_g a + k_1} C - \frac{\rho_s k_2 k_g a}{k_g a + k_1} S. \tag{6}$$

Equations (1) and (6) are the basic expressions which will be used to relate the adsorbate concentration in the gas and solid phases to time and distance. The greatest limitations to these equations are that adsorption must occur from a dilute gas stream, and internal diffusion into the solid particles cannot be represented. To include internal diffusion as a rate controlling mechanism, however, can be accomplished by assuming a geometrical configuration of the adsorbent particles (usually a spherical shape). The mathematical approach for this case is available in the literature (22).

The initial and boundary conditions applicable for a fixed-bed operation are

Initial Condition: $C = \bar{C} = S = 0,\ z = z,\ \theta < 0$

Boundary Condition: $C = C_o,\ z = 0,\ \theta > 0,$

where C_o = inlet concentration of adsorbate, $\frac{\text{g-mole}}{\text{liter}}$.

Before proceeding, the generality of this mathematical model can be shown by considering two formulations. In the first, the only controlling mechanism in the adsorption process is assumed to be mass transfer of the adsorbate from the bulk gas stream to the stagnant gas film. Here equilibrium exists between the adsorbate molecules on the solid surface and those in the stagnant film and can be represented by the relation

$$S = \lambda \bar{C} \tag{7}$$

where

λ = Equilibrium constant, liter/g mole solid.

The gas phase and the gas film and solid phase equations are unaffected but the solid phase mass balance is replaced by the equilibrium expression, Equation (7). Combining Equation (7) with Equation (4) results in

$$\rho_s \frac{\partial S}{\partial \theta} = k_g a C - \frac{k_g a}{\lambda} S \tag{8}$$

which can be used with Equation (1) to represent the adsorption process under the given assumption.

In the second consideration, the only rate controlling mechanisms are adsorption and desorption with equilibrium between the adsorbate molecules in the bulk gas stream and those in the stagnant gas film. The equilibrium expression now is written as

$$\bar{C} = \beta C \tag{9}$$

where

β = Equilibrium constant, dimensionless

Equation (9) can be substituted directly into Equation (3) to yield

$$\rho_s \frac{\partial S}{\partial \theta} = k_1 \beta C - \rho_s k_2 S \tag{10}$$

which can be used in conjunction with Equation (1) to represent the adsorption process governed by the above assumption. By comparison of the solid phase Equations (6), (8), and (10) it is obvious that they are all of the form

$$\frac{\partial S}{\partial \theta} = f'C - gS \tag{11}$$

where f' and g can have any of the following representations:

I. $f' = \frac{1}{\rho_s} \frac{k_1 k_g a}{k_g a + k_1}$ $\qquad g = \frac{k_2 k_g a}{k_g a + k_1}$

II. $f' = \frac{k_g a}{\rho_s}$ $\qquad g = \frac{k_g a}{\rho_s \lambda}$

III. $f' = \frac{k_1 \beta}{\rho_s}$ $\qquad g = k_2$

The gas phase equation for all three conditions is represented by Equation (1). The generality of the model is thus confirmed by the similarity of the solid phase equations to Equation (11) which is representative of any of three rate controlling mechanisms and the gas phase expression, Equation (1), which remains the same regardless of the rate controlling resistances.

The subsequent developments will be based primarily on Equations (1) and (6), but will be equally applicable to any of the rate controlling cases mentioned.

Simultaneous solution of Equation (1) and (6) require the aid of finite difference calculus since analytical solutions are unavailable. The methods employed are quite common in the literature (23) and therefore only a brief description of the reduction of the differential equations to finite difference equations will be discussed.

Equation (1) can be changed to a more suitable form for computer solution by combining Equation (1) with Equation (4) to eliminate the term $k_g a(C-\bar{C})$ and dividing both sides of the resultant equation by C_o, the inlet adsorbate concentration. The ensuing expression is

$$\frac{\partial C}{\partial \theta} = \frac{D_g}{\epsilon} \frac{\partial^2 C}{\partial z^2} - \frac{u}{\epsilon} \frac{\partial C}{\partial z} - \frac{\rho_s}{C_o \epsilon} \frac{\partial S}{\partial \theta} \qquad (12)$$

where C now represents the normalized concentration C/C_o.

Dividing both sides of Equation (6) by C_o leads to the corresponding solid phase equation

$$\frac{\partial S}{\partial \theta} = \frac{C_o}{\rho_s} \frac{k_1 k_g a}{k_g a + k_1} C - \frac{k_2 k_g a}{k_g a + k_1} S \qquad (13)$$

To solve Equations (12) and (13) simultaneously on an analog computer, it is only necessary to reduce Equation (12) to an ordinary differential equation. Through application of finite difference calculus, Equation (12) can be reduced to the finite difference or ordinary differential equation

$$\frac{\partial C_i}{\partial \theta} = \left(\frac{D_g}{\epsilon \Delta z^2} - \frac{u}{2\epsilon \Delta z}\right) C_{i+1} - \frac{2D_g}{\epsilon \Delta z^2} C_i$$

$$\left(\frac{D_g}{\epsilon \Delta z^2} + \frac{u}{2\epsilon \Delta z}\right) C_{i-1} - \frac{\rho_s}{C_o \epsilon} \frac{\partial S_i}{\partial \theta} \qquad (14)$$

where the subscript i refers to a particular location in the fixed-bed. The corresponding finite difference form of Equation (13) is

$$\frac{\partial S_i}{\partial \theta} = \frac{C_o}{\rho_s} \frac{k_1 k_g a}{k_g a + k_1} C_i - \frac{k_2 k_g a}{k_g a + k_1} S_i \qquad (15)$$

If the fixed-bed is divided into n equally spaced sections or modules labeled i = 0 to i = n, the absorbate concentration at any module i at any particular instant can be obtained from a knowledge of the concentration at the

$i + 1$ and $i - 1$ modules at the same period in time. Module 0 refers to the inlet position in the column and n, the outlet. Since Equations (14) and (15) are readily solved on an analog computer, the problem is to develop a computer program to simultaneously solve two ordinary differential equations at each module. The number of modules used is dependent upon the size of the computer and/or the accuracy of the solution desired.

The programming of Equations (14) and (15) requires some minor alterations. The length of an actual adsorption experiment can be as much as 300 min. This period of time cannot be simulated as such in a computer solution but must be altered by the scaling equation

$$t = \frac{\theta}{100} \tag{16}$$

which says that the computer time t will be 100 times as fast as the actual experimental time θ. After substitution of Equation (11) into Equation (14) and (15), it was found that for the calculated values to remain within the computer limits, both sides of Equations (14) and (15) had to be divided by 100. The result of these alterations leads to the actual equations which were used to represent the fixed-bed adsorption process on an analog computer. The gas phase equation is now

$$10^{-2}\ \frac{\partial C_i}{\partial t} = \left(\frac{D_g}{\epsilon \Delta z^2} - \frac{u}{2\epsilon \Delta z}\right) C_{i+1} - \frac{2D_g}{\epsilon \Delta z^2} C_i + \left(\frac{D_g}{\epsilon \Delta z^2} + \frac{u}{2\epsilon \Delta z}\right) C_{i-1} - \frac{\rho_s}{C_o \epsilon} 10^{-2}\ \frac{\partial S_i}{\partial t} \qquad (17)$$

and the solid phase equation,

$$10^{-2}\ \frac{\partial S_i}{\partial t} = \frac{C_o}{\rho_s}\ \frac{k_1 k_g a}{k_g a + k_1} C_i - \frac{k_2 k_g a}{k_g a + k_1} S_i \qquad (18)$$

The analog computer program for simultaneous solution of Equations (17) and (18) which represent the first n-1 sections of the fixed-bed can be seen in Figure 6. To simplify the reading of Figure 6, the following definitions were employed. There were

$$b' = D_g/\epsilon \Delta z^2$$

$$d' = \frac{u}{2\epsilon \Delta z}$$

$$e = \rho_s/C_o \epsilon$$

$$f = f' C_o$$

and g has the same meanings as previously defined.

The calculation of the adsorbate concentration at the nth module requires a slightly different finite difference treatment of Equations (12) and (13) since the concentration

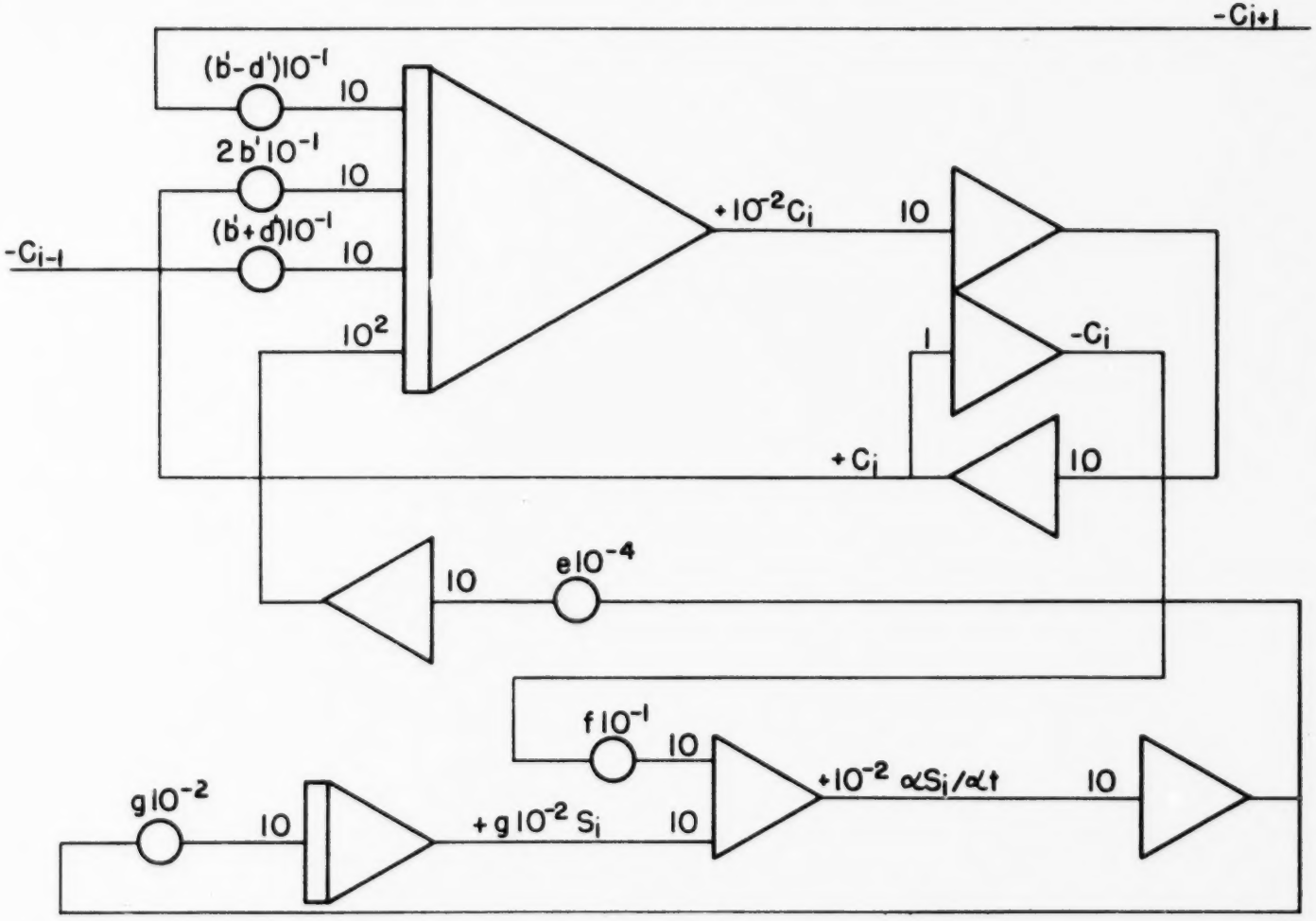

FIGURE 6

GENERAL ANALOGUE COMPUTER PROGRAM

at the n + 1 module is unknown. For this treatment reference to the literature (23) is made once again and only the final finite difference form of these equations will be presented. The adsorbate concentration at the nth module, therefore, can be obtained by simultaneous solution of the gas phase equation

$$10^{-2}\frac{\partial C_n}{\partial t} = \left(\frac{D_g}{\epsilon \ell z^2} - \frac{3u}{2\epsilon\Delta z}\right) C_n - \left(\frac{2D_g}{\epsilon\Delta z^2} - \frac{4u}{2\epsilon\Delta z}\right) C_{n-1}$$

$$+ \left(\frac{D_g}{\epsilon\Delta z^2} - \frac{u}{2\epsilon\Delta z}\right) C_{n-2} - \frac{\rho_s}{C_o \epsilon} 10^{-2} \frac{\partial S_n}{\partial t} \qquad (19)$$

and the solid phase equation

$$10^{-2}\frac{\partial S_n}{\partial t} = \frac{C_o}{\rho_s} \frac{k_1 k_g a}{k_g a + k_1} - \frac{k_2 k_g a}{k_g a + k_1} S_n . \qquad (20)$$

The analog computer program for these equations is presented in Figure 7. The definitions of b', d', e, f, and g have been used similarly, as before. The theory of analog computers may be found elsewhere (29).

It should be noted that the maximum value of n employed in this study was 5. This was required since only 48 integrating circuits were available on the Model AD-2-64PPC Applied Dynamics computer.

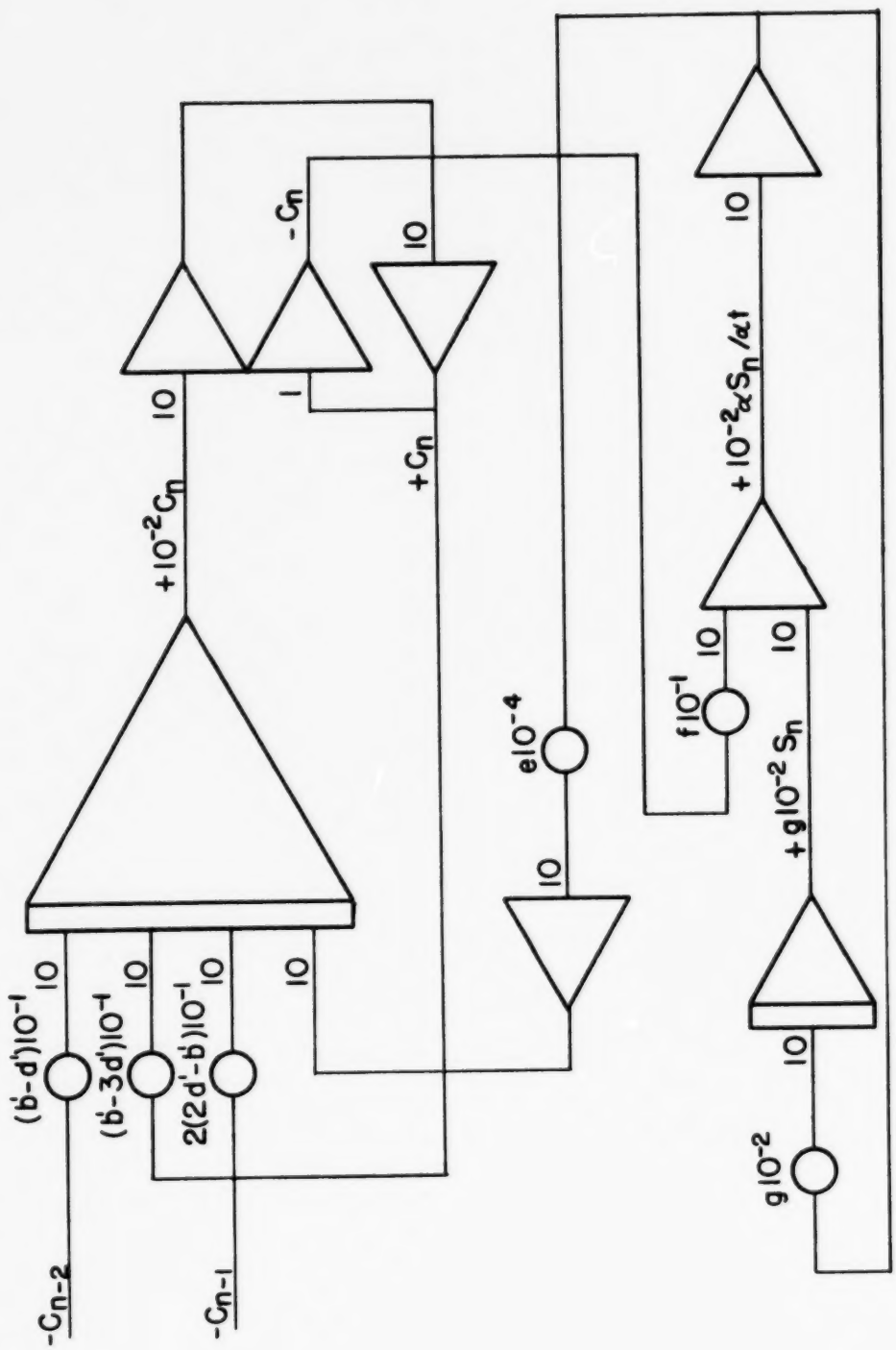

FIGURE 7

END CONDITION ANALOGUE COMPUTER PROGRAM

THEORETICAL RESULTS

Since the mathematical model for the fixed-bed adsorption process applies for operations at low inlet adsorbate or HCl concentrations, the data from the experimental series 9, 11, and 13 were chosen for the model studies. These experimental runs correspond to inlet HCl mole fractions of 0.102, 0.076, and 0.128. The normalized output gas stream concentration versus time representations for the experimental data are illustrated in Figures 8, 9, and 10 along with the theoretical curves obtained from the analog computer solutions of the mathematical model.

The values of the model parameters b, d, e, f, and g which have the desired agreement between the theoretical and experimental curves are listed in Table II. The parameters b and d have the representation

$$b = \frac{D_g}{\epsilon}$$

$$d = \frac{u}{\epsilon}$$

The numerical values of b, d, and f were maintained constant at 0.366 cm/sec, 1.72 cm/sec, and 0.30 liter/g.mole solid-sec, respectively, for each of the experimental sets of data except where d was set equal to zero and b to 0.160 cm/sec. The value of the parameter e varied from 3200 to 1900 $\frac{\text{g.mole solid}}{\text{g.mole HCL}}$, and g, from 0.600 to 0.400/sec.

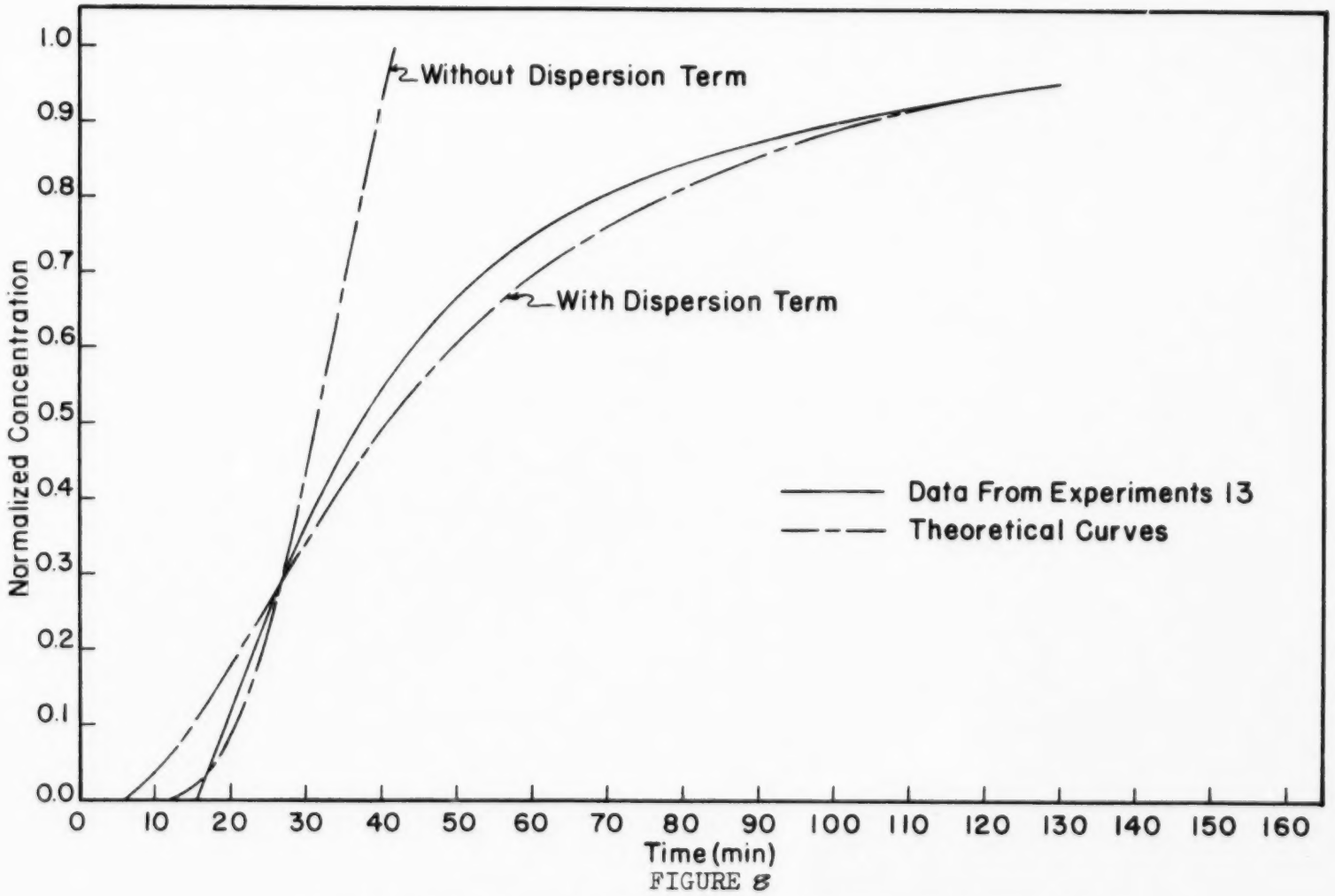

FIGURE 8

EXPERIMENTAL AND THEORETICAL CONCENTRATION HISTORIES A

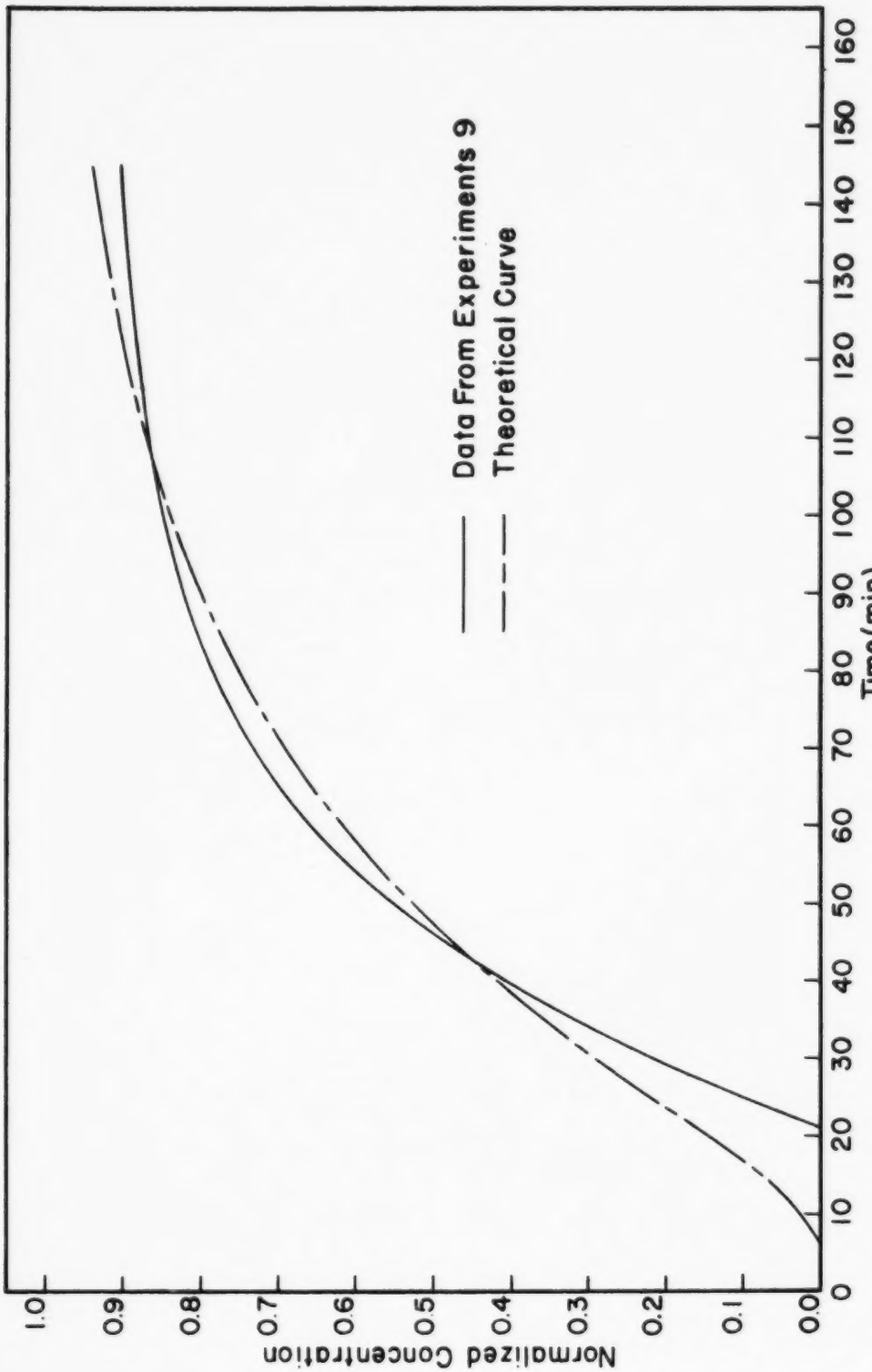

FIGURE 9

EXPERIMENTAL AND THEORETICAL CONCENTRATION HISTORIES B

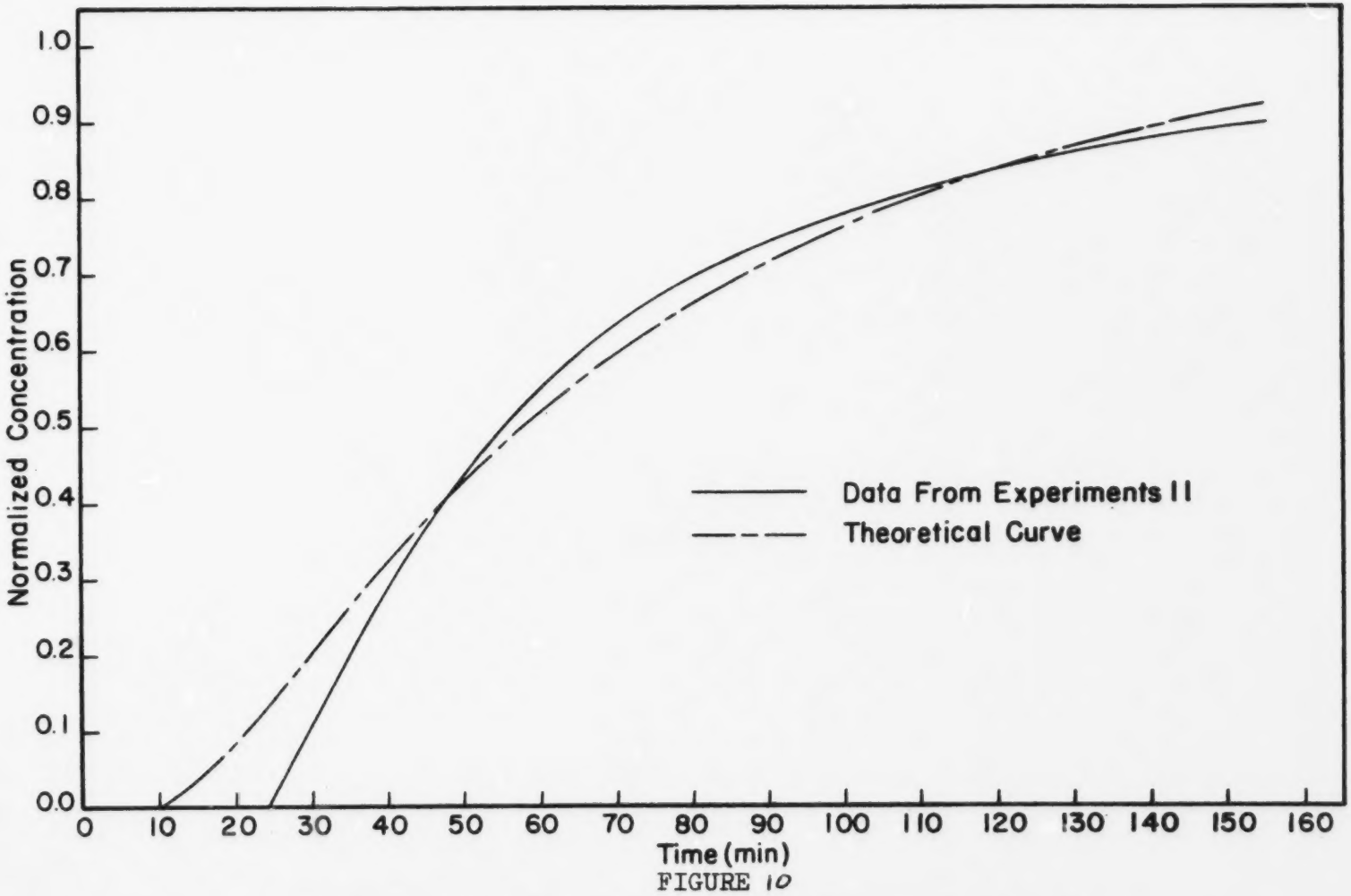

FIGURE 10

EXPERIMENTAL AND THEORETICAL CONCENTRATION HISTORIES C

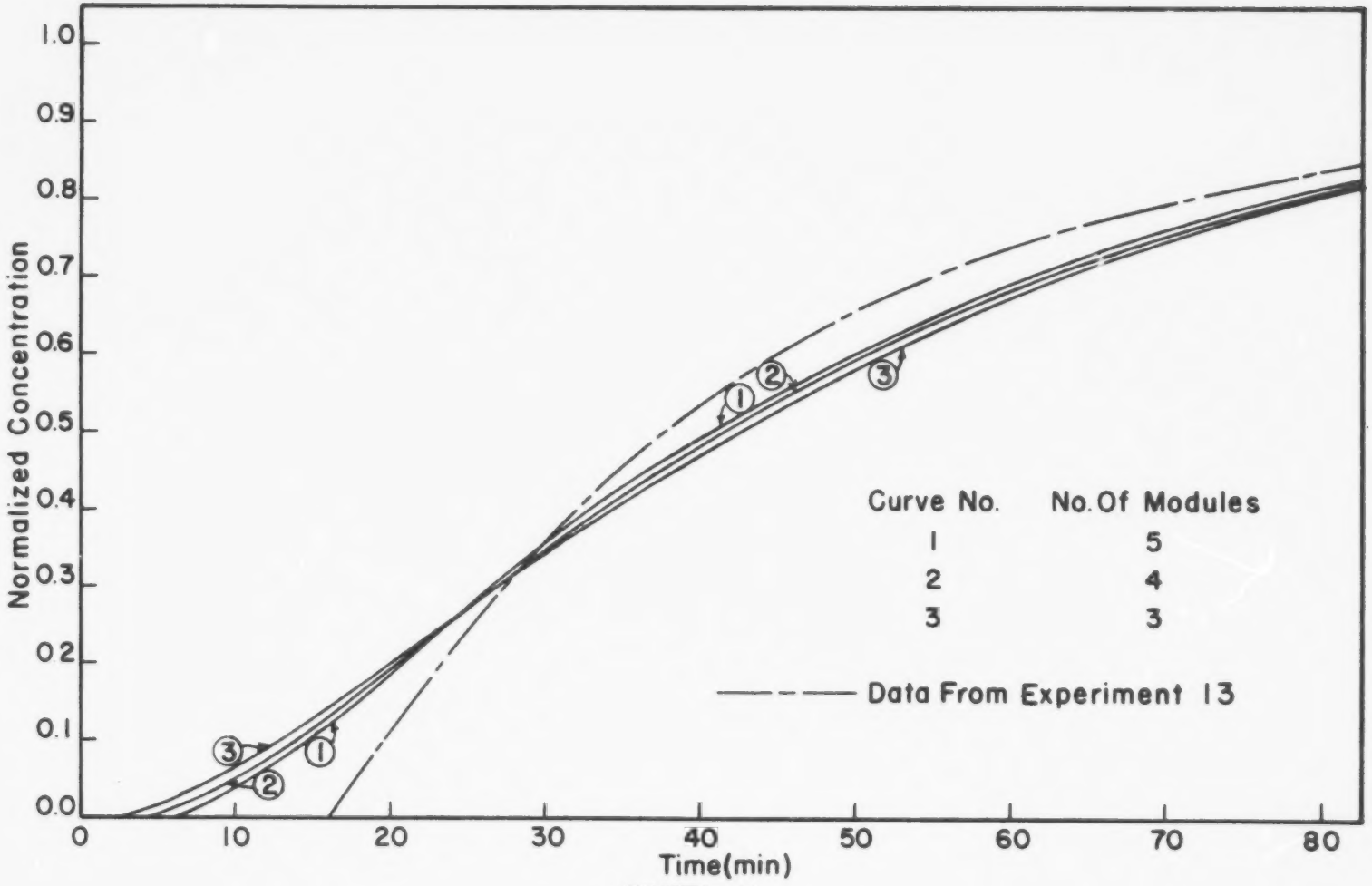

FIGURE 11

EFFECT OF COMPUTER MODULES ON THEORETICAL RESULTS

TABLE 2

VALUES OF THE MATHEMATICAL MODEL PARAMETERS

Experiment	b $\left(\frac{cm^2}{sec}\right)$	d $\left(\frac{cm}{sec}\right)$	e $\left(\frac{\text{g-mole solid}}{\text{g-mole HCl}}\right)$	f $\left(\frac{\text{liter}}{\text{g-mole solid-sec}}\right)$	g $\left(\frac{1}{sec}\right)$
9	0.366	1.72	1900.	0.030	0.440
11	0.366	1.72	3200.	0.030	0.600
13	0.366	1.72	1300.	0.030	0.353
13	0.160	0.00	1300.	0.030	0.353

ANALYSIS OF THEORETICAL RESULTS

The determination of the parameters b, d, e, f, and g in the theoretical mathematical model of the fixed-bed adsorption process included both a trial and error procedure and estimates from experimental data. The parameters which were estimated prior to the trial and error adjustments of the adsorption model to the experimental data were e and the ratio f/g. To determine the value of e, the proper C_o and ϵ had to be known. Since C_o and ϵ could be calculated from the experimental data, the quantity e was estimated. The ratio f/g is essentially the equilibrium adsorption value for a particular set of experimental conditions. This arises from considering that the $\frac{\partial S}{\partial \theta}$ in Equation (11) is equal to zero when equilibrium adsorption is obtained. Therefore, if the right-hand side of Equation (11) is set equal to zero and solved for S, the result is

$$S = \frac{f'}{g} \cdot C. \tag{21}$$

If Equation (21) is normalized by dividing both sides by C_o, the value of S is given by

$$S = \frac{C_o f'}{g} \cdot C \tag{22}$$

where C now represents the normalized quantity C/C_o. Since C is normalized, the final value of S is given by the ratio

$\frac{f}{g}$. An estimate of this ratio can be obtained from the equilibrium concentration of hydrogen chloride in the solid phase for a particular experiment.

The parameters b and d, therefore, were essentially the only completely unknown values. However, the superficial linear velocity U is contained in the parameter d, and, therefore, it was estimated by setting b equal to zero in the initial attempts to fit the mathematical model to the experimental data. The velocity term was varied until an approximate fit of the theoretical equations to the experimental data was obtained. Such a solution was found to predict the initial 30 to 40 percent of the adsorption curves quite satisfactorily as illustrated in Figure 8 but was unable to provide the tailing which occurred in the real process. This solution would be the same as that obtained by the model proposed by Marshall and Hougen (11). To obtain the tailing effect the parameter d, which contains the back-mixing or dispersion coefficient, was introduced. The values of b and d were then varied with small modifications of e, f, and g until the desired mathematical solutions were obtained.

The experimental data from series 13 was chosen as the first to be modeled and the results are presented in

Figure 8. Series 9 and then 11 were subsequently modeled as shown in Figures 9 and 10.

The solutions to the mathematical model were found to predict the upper 80 percent of the experimental adsorption curves quite accurately. The greatest deviations from these curves were obtained in the prediction of the outlet gas stream concentration from a value of zero to a normalized value of 0.30. The breakthrough times were found to vary as much as 67 percent, an error which decreased to a maximum of 10.3 percent for the time required to reach a normalized exit stream concentration of 0.30. The errors in this region were always such that the hydrogen chloride concentration in the exit stream was predicted prematurely high at a given time.

A similar comparison between the experimental data of Series 13 and the corresponding solution of the theoretical model with the back-mixing coefficient equal to zero gives an error between the predicted and actual breakthrough time of 25 percent and decreases to an error of zero for the time required to reach a normalized exit concentration of 0.30. However, from this point on the difference between the predicted and actual effluent gas concentration increases rapidly as shown in Figure 8. Hence, the model neglecting

back-mixing was found to predict the initial 40 percent of the experimental curve. It was felt, however, that a better fit to the experimental data was obtained by using the dispersion term in the mathematical model.

The calculated values of the porosity factor, ϵ, the equilibrium adsorption content, E, the back-mixing coefficient, D_g, the superficial linear velocity, u, the mass transfer coefficient times the interfacial area, $k_g a$, the forward adsorption rate constant times the gas phase stagnant film equilibrium constant, $k_1\beta$, and the reverse rate desorption constant, k_2, from the parameters b, d, e, f, and g are presented in Table III. It should also be noted that the values $k_g a$, k_1, and k_2, for the general three rate-controlling resistances could not be obtained since there were only two independent equations and three unknowns. To calculate these values it would have been necessary to conduct static studies under the same operating conditions as the flow experiments, thereby determining k_1 and k_2 from Equation (3). The values of $k_g a$ could then be obtained from the solid phase parameters used in the corresponding flow experiments. Hence, the values of $k_g a$ apply only to the model which employs a gas film resistance and $k_1\beta$ and k_2 to the adsorption-desorption resistance case.

TABLE 3

THEORETICAL QUANTITIES FROM MODEL PARAMETERS

Experiment	*ϵ	$E\left(\frac{\text{g mole HCl}}{\text{g mole solid}}\right)$	$D_g\left(\frac{cm^2}{sec}\right)$	$u\left(\frac{cm}{sec}\right)$	$k_g a\left(\frac{1}{sec}\right)$	$k_1{}^{\beta}\left(\frac{1}{sec}\right)$	$k_2\left(\frac{1}{sec}\right)$
13	0.177	0.085	0.0549	0.1258	6.90	6.90	0.353
9	0.152	0.063	0.0549	0.1258	8.65	8.65	0.440
11	0.121	0.040	0.0549	0.1258	11.62	11.62	0.600

*ϵ = 0.15 for all other calculations

The theoretical porosity factors were found to vary from 0.177 to 0.121 with an average value of 0.150. This corresponded to a deviation about the average of $\pm$ 18 per cent. This value is comparable to the estimated value of 0.19 and is reasonable considering the small particle size of the solid.

The experimental equilibrium values were 0.085, 0.068, and 0.050 g-moles HCl/g-mole solid as compared to the theoretical estimates of 0.085, 0.063, and 0.040 g-moles HCl/g-mole solid. The percentage errors were 0.0, 7.95, and 25.0 percent, respectively. The variation between the theoretical and experimental equilibrium contents should be considered in terms of the approximate methods used to obtain the experimental values and their numerical smallness which leads to large percentage errors for only small differences.

The dispersion coefficient and superficial linear velocity remained constant for each set of data at respective values of 0.0549 cm^2/sec, and 0.0258 cm/sec. Such behavior is consistent with the theoretical considerations of the back-mixing coefficient and the assumption that the loss of adsorbate from the gas stream does not appreciably affect the over-all velocity of the mixture.

For the case in which mass transfer across a gas film is the only controlling resistance, the term $k_g a$ was found to be 6.90, 8.65, and 11.62/sec. for the respective experimental Series 13, 9, and 11. Since $k_g a$ is common to both parameters f and g, it was possible to calculate $k_g a$ from the given value of f, C_o and ρ_s for each set of data. Using this value of $k_g a$ and the known values of g, and ρ_s, it was possible to calculate the equilibrium constant, λ . The value of λ can also be estimated from the experimental data. Comparison of the values of λ obtained from theoretical and experimental considerations provides a means by which the proposed mechanism of mass transfer in this case can be tested. The experimental value of λ was estimated to be 20.4 $\frac{\text{liter}}{\text{g mole solid}}$, while the theoretical calculations gave values of 15.9, 15.7, and 15.8 $\frac{\text{liter}}{\text{g mole solid}}$ for the experimental Series 9, 11, and 13, respectively. The theoretical values were all within 23.2 percent of the experimentally determined equilibrium constant.

The values of $k_1\beta$ were 6.90, 8.65, and 11.62/sec. with corresponding values of k_2 of 0.353, 0.440, and 0.660/sec. These terms applied when the mathematical model incorporated the adsorption-desorption resistances to mass transfer. The values of these constants should be the same as those obtained from static studies of the adsorption under

similar operating conditions as the corresponding flow experiments. These data were unavailable, however, and the proposed mechanism of mass transfer could not be tested as in the above case.

The initial part of the experimental curve was found to remain at zero concentration until the breakthrough time arrived, after which a subsequent rapid rise in concentration occurred. The prediction of such behavior by the mathematical model was felt to be attainable through the use of more finite difference modules or increments. Since the size of the computer available limited the number of modules to five, the effect of a larger number of modules on the theoretical solutions could not be determined. However, the effect of using a fewer number was studied for each of the Series 9, 11, and 13. The results are shown in Figure 11, with the presentation of the theoretical solutions for the experimental Series 13.

It is seen that as the number of modules was decreased from five to four to three, the breakthrough times decreased significantly. When the normalized effluent gas stream concentration reached about 0.25 the curves crossed over with the three module approximation being the farthest from the experimental curve, the four module next, and the five module

the closest. As the normalized concentration reached about 0.90 the curves converged to one. From these observations, it can be concluded that the use of more modules tends to increase the breakthrough time, provide initially a more rapid rise in the adsorption curve, and finally, converge to the upper portion of the curves obtained in this study. Whether or not the theoretical solution would eventually converge completely on the experimental curve with an increased number of modules is a problem which would best be solved using a digital computer or a larger analog.

The use of a digital computer would essentially eliminate those errors encountered with the analog because of the great variation in the numerical values of the theoretical parameters and the inherent inaccuracy in certain operating regions of the computer. The numerical range in the parameters made impossible the setting of several of the computer adjustments to the desired accuracy. Evidence of this error was indicated when the outlet gas concentration reached a constant value which many times was either greater or less than the input. In these cases the output was adjusted to record at the inlet value. The extent of the error incurred by such procedure is questionable.

The inherent inaccuracy of the computer would be most evident in the low concentration regions where a zero output concentration must be maintained until the breakthrough time. Such response is unlikely since very stringent operating characteristics on the electronic tubes is required. This effect on the computer solutions is also questionable but must be assumed significant.

The nearness of the solution of the finite difference approximation to the actual solution of the differential equations is quite difficult to estimate. The usual procedure is to increase the number of increments and observe the difference or convergence in the solutions. Whenever the difference becomes insignificant or convergence is essentially complete, the necessary accuracy is assumed to have been attained. In view of the inaccuracies previously mentioned and the fact that the finite difference solution is considered adequate in the upper 80 percent of the exit gas stream concentration range, such procedure would not conclusively indicate the errors involved from an inadequate number of increments.

Hence, the inaccuracies in the theoretical solutions cannot be conclusively interpreted and must be evaluated in future studies where digital computer applications seem to be warranted.

CONCLUSIONS

The adsorption of gases on fixed-beds can exhibit a tailing effect, which requires long times for the exit gas concentration to reach the entering concentration. This effect can be described by equations involving axial dispersion in the gas phase.

The adsorption of hydrogen chloride on chromium oxinate exhibits the properties of physical adsorption as determined by observation of adsorption-desorption curves.

ACKNOWLEDGMENT

The authors wish to thank the Public Health Service, Bureau of State Services, Division of Air Pollution, for part of the support for this work through grant #AP-00325.